Method to study cell migration under uniaxial compression

Nishit Srivastava[a], Robert R. Kay[b], and Alexandre J. Kabla[a,*]
[a]Department of Engineering, University of Cambridge, Cambridge CB2 1PZ, United Kingdom; [b]MRC Laboratory of Molecular Biology, Cambridge CB2 0QH, United Kingdom

ABSTRACT **The chemical, physical, and mechanical properties of the extracellular environment have a strong effect on cell migration. Aspects such as pore size or stiffness of the matrix influence the selection of the mechanism used by cells to propel themselves, including by pseudopods or blebbing. How a cell perceives its environment and how such a cue triggers a change in behavior are largely unknown, but mechanics is likely to be involved. Because mechanical conditions are often controlled by modifying the composition of the environment, separating chemical and physical contributions is difficult and requires multiple controls. Here we propose a simple method to impose a mechanical compression on individual cells without altering the composition of the matrix. Live imaging during compression provides accurate information about the cell's morphology and migratory phenotype. Using *Dictyostelium* as a model, we observe that a compression of the order of 500 Pa flattens the cells under gel by up to 50%. This uniaxial compression directly triggers a transition in the mode of migration from primarily pseudopodial to bleb driven in <30 s. This novel device is therefore capable of influencing cell migration in real time and offers a convenient approach with which to systematically study mechanotransduction in confined environments.**

Monitoring Editor
Margaret Gardel
University of Chicago

Received: Aug 9, 2016
Revised: Dec 6, 2016
Accepted: Jan 17, 2017

INTRODUCTION

Cell migration is an important part of both healthy and pathological biological processes. During embryo development, wound healing, or immune response, cells have to navigate through complex environments to shape tissues or perform their physiological function (Martin, 1997; Miller and Davidson, 2013; Bonnans *et al.*, 2014). Cell migration is also a defining feature of cancer metastasis (Friedl and Gilmour, 2009). However, any understanding of in vivo cell migration relies on our ability to study how cells perceive and respond to the chemical and mechanical cues from the environment (Eyckmans *et al.*, 2011). It is well established that many biochemical cues directly influence the behavior of a cell (Alberts *et al.*, 2002). However, mechanical aspects are only starting to be characterized and understood (Charras and Sahai, 2014), especially in the context of the three-dimensional (3D) environment. The specific properties of the mechanical environment—in particular its stiffness and confining effect—directly influence single-cell migration and collective invasion of cells (Bergert *et al.*, 2012; Vedula *et al.*, 2012; Paluch and Raz, 2013; Tozluoglu *et al.*, 2013; Wolf *et al.*, 2013). Cells can sense a variety of external mechanical signals that interact with proteins such as integrin, paxillin, and other signaling molecules in the cytoplasm such as Rho and Rho-associated kinases (Chen *et al.*, 2004; Lämmermann and Sixt, 2009; Gardel *et al.*, 2010; DuFort *et al.*, 2011; Abu Shah and Keren, 2013; Charras and Sahai, 2014). There is, however, a lack of quantitative understanding of how different mechanotransductive pathways operate in a cell in order to sense mechanical information and how they control key biophysical quantities such as membrane tension, membrane–cortex attachment, or actin polymerization that regulate cell migration (Houk *et al.*, 2012; Tyson *et al.*, 2014). Furthermore, we need to study such mechanisms in realistic conditions, accounting for the mechanical resistance that a natural environment would provide to cell migration. A simple quasi-3D model system with tunable mechanical characteristics would enable a systematic study of cells' migratory response to mechanical stimuli.

This article was published online ahead of print in MBoC in Press (http://www.molbiolcell.org/cgi/doi/10.1091/mbc.E16-08-0575) on January 25, 2017.

*Address correspondence to: Alexandre J. Kabla (ajk61@cam.ac.uk).

Abbreviations used: ADC, analogue-to-digital converter; cAMP, adenosine 3′,5′-cyclic monophosphate.

Current experimental techniques to study cell mechanics include local methods such as optical or magnetic tweezers (Neuman and Nagy, 2008; De Vlaminck and Dekker, 2012), cantilevers (Bufi *et al.*, 2015), and micropipette aspiration (Dai *et al.*, 1999). These techniques offer a convenient way to impose a force on individual cells but are not well suited to the study of migratory cells, which would rapidly move away from the probe. Soft substrates have been used extensively to study force generation and cell rheology (Harris *et al.*, 1980), particularly in combination with traction force microscopy techniques (Krishnan *et al.*, 2009). These tools largely rely on cells being plated on a flat substrate and cannot properly examine cell migration in 3D environments and how the cells respond to cues such as a compressive stress (rather than imposed deformations).

Microfluidic systems and microfabrication techniques are popular approaches to studying the migration of cells in different geometries and mechanical environments (Liu *et al.*, 2015; Denais *et al.*, 2016; Raab *et al.*, 2016) and on different topographical patterns (Kim *et al.*, 2009) and micropillars (Ghassemi *et al.*, 2012; Lam *et al.*, 2012). These techniques have been instrumental in our understanding of the forces and molecular mechanisms required for migration in confined spaces, probing in particular the role of the nucleus during cell migration (Raab *et al.*, 2016). In the case of confinement, the environment inside such devices, however, is much stiffer than most single cells and soft tissues, whose stiffness is typically in the range of 0.1–10 kPa (Discher *et al.*, 2005). Although these are ideal techniques to probe the mechanisms of migration inside preexisting geometrical gaps, they do not fully mimic the broad class of situations in which a cell has to create its path through surrounding tissues (Charras and Sahai, 2014).

Under-agarose assays offer an alternative route to study cell migration and mechanotransduction closer to physiological conditions, in particular in conjunction with cell chemotaxis (Nelson *et al.*, 1975; Laevsky and Knecht, 2001). This technique has been used to study the migration of neutrophils and *Dictyostelium discoideum* cells and allowed an exploration of the key molecular pathways involved in chemical sensing (Kay *et al.*, 2008; Nichols *et al.*, 2015). In such assays, the mechanical properties of the hydrogel can be tuned to study its effect on cell migration. Zatulovskiy *et al.* (2014) showed that *D. discoideum* cells switch from a pseudopodial mode of migration to bleb mode when the stiffness of the hydrogel is increased. In such experiments, modulation of the stiffness is achieved by changing the gel concentration and hence the pore size and chemical composition of the environment (Normand *et al.*, 2000). It is therefore possible that the stiffness is not a primary parameter controlling the mode of cell migration during such under-agarose assays. Instead of tuning the stiffness of the gel, a mechanical load could be used to modulate the mechanical environment around the cells. King *et al.* (2011), for instance, applied known weights on a slab of agarose gel to probe the role of pressure on autophagy in *Dictyostelium*. In this study, we extend this approach and build an experimental system designed to dynamically impose a mechanical load on a cell migrating under an agarose layer. Because load and gel concentration are controlled independently, the contributions of the matrix stiffness (or composition) and load can be separated. Specifically, we show that a compressive load on *Dictyostelium* can be used to control the mode of cell migration under agarose and open the way to a systematic study of the transduction pathways involved.

RESULTS

Device design

The primary goal of the device, referred to as the cell squasher in this article, is to apply a steady and uniform compressive stress on a slab of hydrogel while simultaneously performing high-resolution live imaging of cells squashed between the gel and a glass coverslip. The overall design of the device is shown in Figure 1. A rectangular plunger (Perspex, typically 4 mm wide, 10 mm long, and 3 mm thick) is used to compress the upper surface of the gel. The vertical position of the plunger is controlled using a motorized translational stage (Newport, TRA-25CC, range 25 mm) so that the load can be dynamically controlled. The pressure imposed by the plunger on the gel is measured by a tension-compression load cell. The horizontal position of the plunger relative to the hydrogel can be adjusted with two manually controlled linear stages.

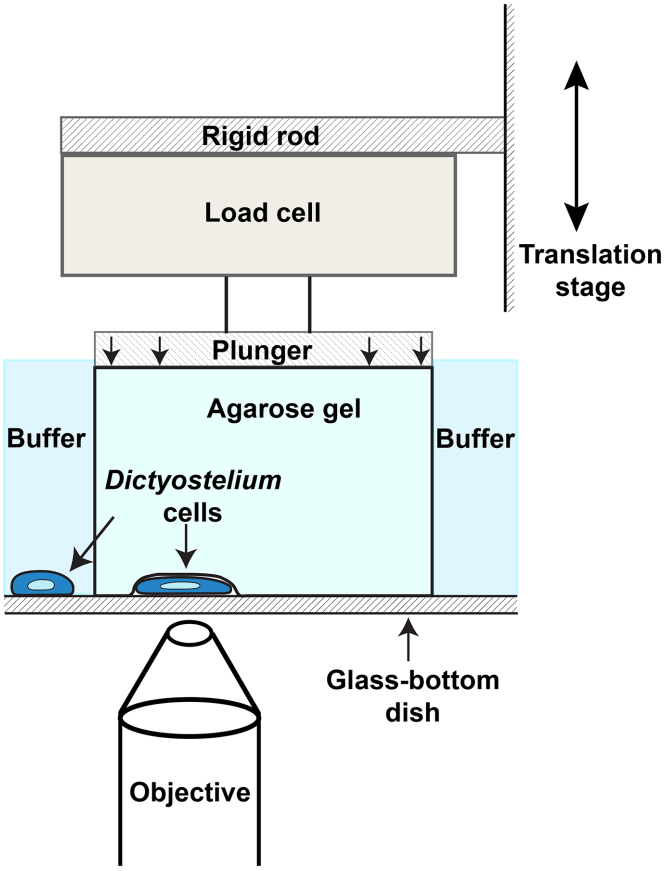

FIGURE 1: Working principle of the cell squasher. A mechanical load is applied uniformly on a hydrogel while cells are migrating underneath the gel in a classical under-agarose assay. The plunger's vertical position is controlled by an automated translation stage. The pressure applied is monitored with a load cell feeding back to the stage control system to ensure an accurate and dynamic control of the loading conditions.

The plunger, load cell, and positioning system with its motorized actuator need to reside on the stage of the microscope (Zeiss LSM780; 160 mm long and 110 mm wide) so that both move together as a combined unit while regions to image are selected. The stage can bear loads up to 60 N. As a result, the cell squasher is designed to be as compact as possible (121.9 mm long, 133.3 mm wide, and 95.2 mm high), making the device fairly portable and usable on a broad range of inverted fluorescence microscopes. The load cell–plunger system also needs to be accommodated between the condenser and lens of the microscope (20 mm apart) along with a reasonable clearance. Only cells expressing fluorescent reporters can be imaged in the reflection mode because this device obstructs transmitted light.

Most of the open-ended questions in the field of cell migration require a range of stress from very small values (25 Pa) to moderate values of the order of few kilopascals (Bao and Suresh, 2003). Over the duration of an experiment (up to a few hours), creep and other time-dependent processes are likely to cause a drop in the compressive load if the plunger is kept stationary (Ahearne *et al.*, 2005). This sets specific requirements for both the sensor and actuator controlling the deformation of the gel.

The system is therefore automated to keep the stress constant within the stated constraints. A mismatch of ~10 Pa in the desired mechanical load is appropriate. Considering a typical gel sample (1% [wt/vol] agarose gels, 2-mm thickness), a 10-Pa change in the mechanical stress corresponds to a plunger displacement of the order of 1 µm. We therefore choose a motorized actuator with a minimum incremental motion of 0.2 µm. The load cell must also be able to sense variations of load of the order of 10 Pa. A Futek sensor, LSB200, and a low-cost 16-bit analogue-to-digital convertor (ADC; Adafruit, ADS 1115) connected to a Raspberry Pi computer provide a required range and precision.

When significant changes in the load are applied (typically at the start of an experiment), a slight drift in the coverslip causes a temporary loss of focus. This is largely due to the compliance of the bottom glass coverslip. The time scale of the load application should be long enough to ensure that the cells are tracked during imposition of load but short enough that the transient response of the cell can be studied. Hence, the stress is ramped up over ~10–20 s (plunger speed of 40 µm/s) so that the focus can be manually adjusted during the plunger motion, keeping cells in focus while recording their transient behavior.

In addition to characterizing cell behavior under compressive load, the same setup can be used to measure the mechanical properties of the gels under which cells migrate. In the next section, we measure the Young's modulus of different agarose gels and compare the performance to a standard indenter system used for material characterization, demonstrating the general application of this system. We then characterize the effect of mechanical load on the migration of cells and quantitatively capture the dynamics of the plasticity in cell migration.

Mechanical characterization of agarose gels

Spherical indentation testing is a standard method to probe the mechanical properties of soft materials (Field and Swain, 1993). Using a spherical indenter as plunger, it is possible to record the force–indentation curve and extract the effective stiffness of the gel in the relevant time scales used in this experiment. Figure 2A shows the variation of force with distance during an indentation test of an agarose gel. As demonstrated in Figure 2B, the force increases with indentation distance according to a power law. Hertz's contact model provides a suitable fit for such indentation curves and allows us to estimate the Young's modulus (Hertz, 1882):

$$F = -\frac{16E_2\sqrt{Rd^3}}{9}$$

where F is the force applied by an indenting bead, E_2 is the Young's modulus of the gel, R is diameter of the bead, and d is the indentation depth. Figure 2C shows the estimated values of the Young's modulus for a range of concentrations (0.5, 0.75, 1, 1.5 and 2%). These are effective values because agarose is not a linear elastic material, and the apparent stiffness depends on the indentation speed due to creep and viscoelastic properties. Nevertheless, we can compare the values obtained with our custom setup with those measured using an industry standard commercial testing machine

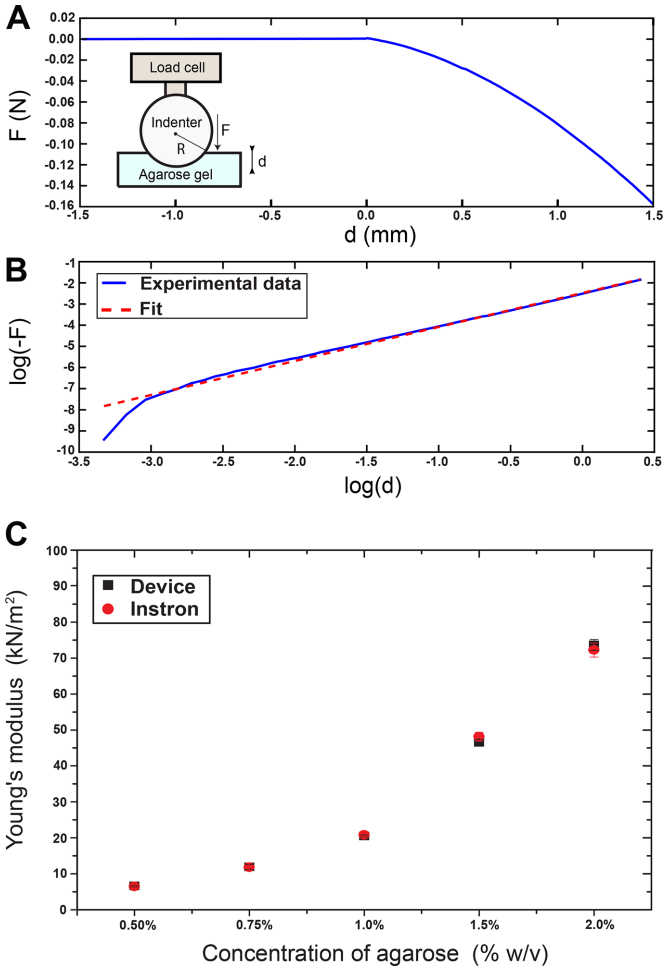

FIGURE 2: (A, B) Force–displacement curve for an indentation with a spherical bead of diameter 6 mm on a 1% (wt/vol) agarose gel of 5-mm thickness. The indent speed is 0.012 mm/s. (B) Fit of the force–displacement curve with the Hertz contact model: $F = -Cd^{3/2}$, where $C = 8.38 \times 10^{-2}$ $Nmm^{-3/2}$. (C) The Young's modulus of agarose gels of different stiffness measured with the custom device and an Instron 5544. For each concentration, two different gels were used, with five different measurements on each gel.

(Instron 5544) as a validation of our measurement pipeline. The values of the Young's modulus obtained from the cell squasher and the Instron are in good agreement (maximal error of 1.9% for stiffer 2% agarose gel). Thus our setup is capable of applying mechanical stress reliably and reproducibly and provides a convenient way to measure the Young's modulus of hydrogels such as agarose with sufficient precision.

Moving back to the flat indenters used to squash the cells under agarose, Figure 3A shows a typical loading curve on a 0.5% agarose gel at 400-Pa load. Initially, the load remains constant as the plunger approaches the agarose gel. The load increases slightly when the plunger comes in contact with the gel due to surface tension between the rectangular plunger and agarose gel surface. It takes ~20 s for the load to reach the desired value. Thereafter the device maintains the load at a constant value, within the 10-Pa precision specified. The device constantly adjusts the position of the plunger, as shown in Figure 3B, to maintain a constant stress by compensating for the creep occurring in the gel. Thus our device can apply a specified load on an agarose gel on a relatively short time scale and is able to maintain it at a constant value over a long duration.

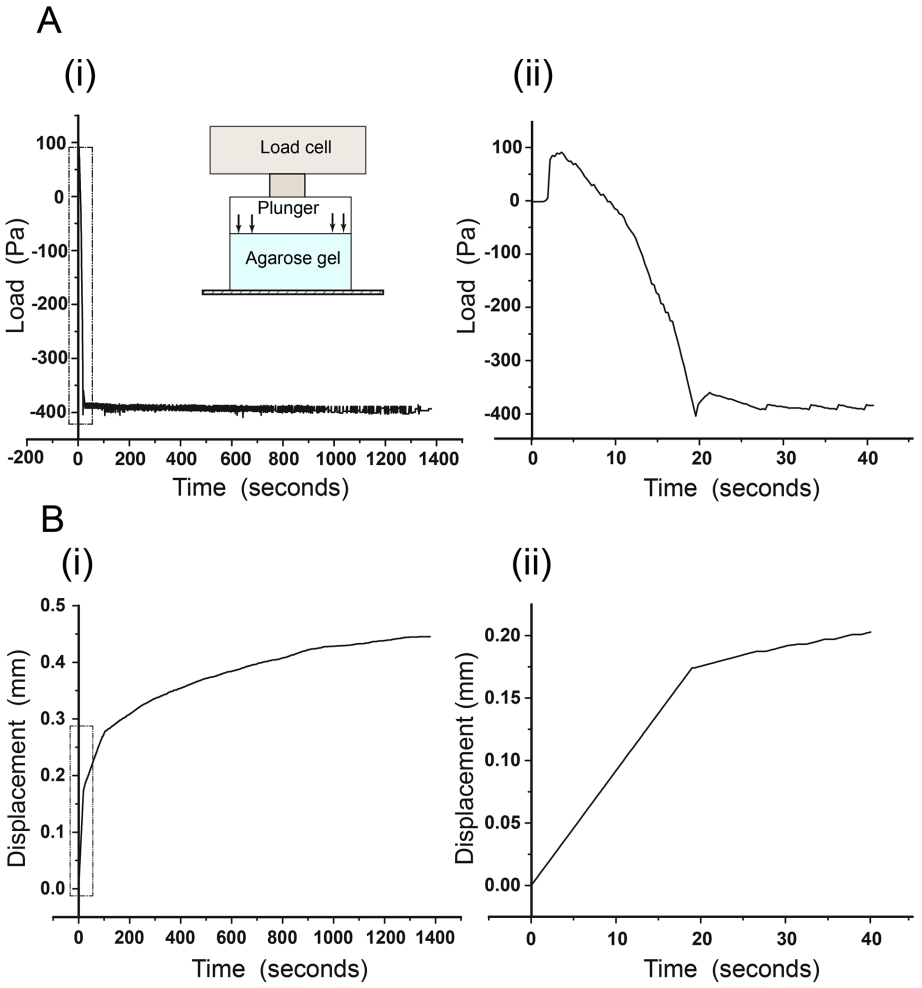

FIGURE 3: Indentation of agarose gel with flat indenter during cell-squashing experiments. (A) Typical loading experiment on a 0.5% agarose gel of 2-mm thickness at 400-Pa load. (i) Variation of load at longer time scales during a typical experiment. (ii) Details of the response during the loading stage. (B) Displacement of the flat indenter for the corresponding loading condition (i) over longer time scales (ii) during the loading stage.

Application to biological experiments

Imposing a compressive load on D. discoideum. To squash cells and probe their response, cells need to be present at an interface between the gel and the glass-bottom dish (Figure 1A). There are two main approaches to achieve this, as illustrated in Figure 4.

Chemotactic cells, such as aggregation-competent *Dictyostelium* cells (cells that have been starved and brought to a state where they will chemotax to cAMP), can be persuaded to migrate under the gel, using a chemoattractant gradient. A conventional setup, an under-agarose assay, involves two independent wells cut in a homogeneous agarose slab of gel, as depicted in Figure 4A. The distance between the wells is 4 mm, and the gel thickness is typically 2 mm. One well is filled with a cell suspension (2×10^5 cells/ml) and the other with a solution of cAMP (5 μM), a strong chemoattractant for *Dictyostelium* cells. After 15–20 min, cells start to respond to the chemotactic gradient and migrate under the agarose slab. Figure 4B depicts the protocol used in such a configuration. The experiment starts without any load applied. Once cells are visible on the microscope under the gel, the plunger imposes a set load on the gel's surface. Alternatively, to probe cells whose migration would not respond to directional cues, cells can be directly squashed by placing a slab of agarose on top of them (Figure 4C). In both cases, once a load is imposed with the plunger, the gel makes contact with the cells and transmits mechanical forces to them, as will be demonstrated.

Effect of a compressive load on D. discoideum. To verify that the cells are effectively compressed by the applied load, we measure their height under a range of compressive stresses on them under 0.5% agarose gel. The height of the cells is quantified by taking *z*-stacks of *Dictyostelium* cells expressing actin-binding domain (ABD)–green fluorescent protein (GFP), which is a reporter for F-actin (Pang *et al.*, 1998). We reconstructed 3D images and measured the distance between the top and bottom of the cells . These *z*-stacks were also corrected for *z*-axis elongation, which occurs as a result of a refractive index mismatch between oil on the microscope lens and aqueous medium of the cells (Traynor and Kay, 2007). As seen in Figure 5, the height of the cells decreased from 7 μm without any load to 3 μm under 400 Pa. A load of 100 Pa was sufficient to squash the cells by 30%. The height seemed to plateau, however, for loads >500 Pa. The data therefore demonstrate that the cell squasher operates in a range of forces appropriate to significantly deform the cells and record their morphological evolution.

Effect of mechanical stress on the migration of cells

In addition to morphological traits, it is also possible to characterize the behavior of the cells and in particular their migration under load. As an example, we studied the transition from pseudopod to bleb-driven migration. Zatulovskiy *et al.* (2014) showed that *Dictyostelium* cells switch to the bleb mode of migration when the stiffness of an agarose layer underneath which they migrate is increased from 0.5 to 2%. We first use the chemoattractant-based assay introduced in Figure 4B with low-concentration (0.5% [wt/vol]) agarose. We indeed observe highly polarized cells migrating toward the gradient of cAMP, using pseudopods as their primary mode of migration (Figure 6A). As soon as a mechanical load of 100 Pa is applied, cells tend to form blebs (Figure 6A and Supplemental Movie S1). This behavior is also observed using the alternative protocol highlighted in Figure 4C without cAMP. Initially, the cells migrate randomly by forming multiple pseudopods in different directions. The application of a compressive load triggers almost instantly the formation of blebs (Figure 6B and Supplemental Movie S2).

We quantified the proportion of blebs among total protrusions formed by the cells to establish the effect of compressive load on protrusion formation. Under no-load conditions and 0.5% agarose gels, blebs formed 25 ± 6.1% of total protrusions, which increased to 66.8 ± 9.4% of total protrusions under 100-Pa steady-state load. Along with transition in type of protrusion, the speed of cells also decreased, from 0.26 μm/s under no-load conditions to 0.18 μm/s under 100-Pa load (Figure 6C).

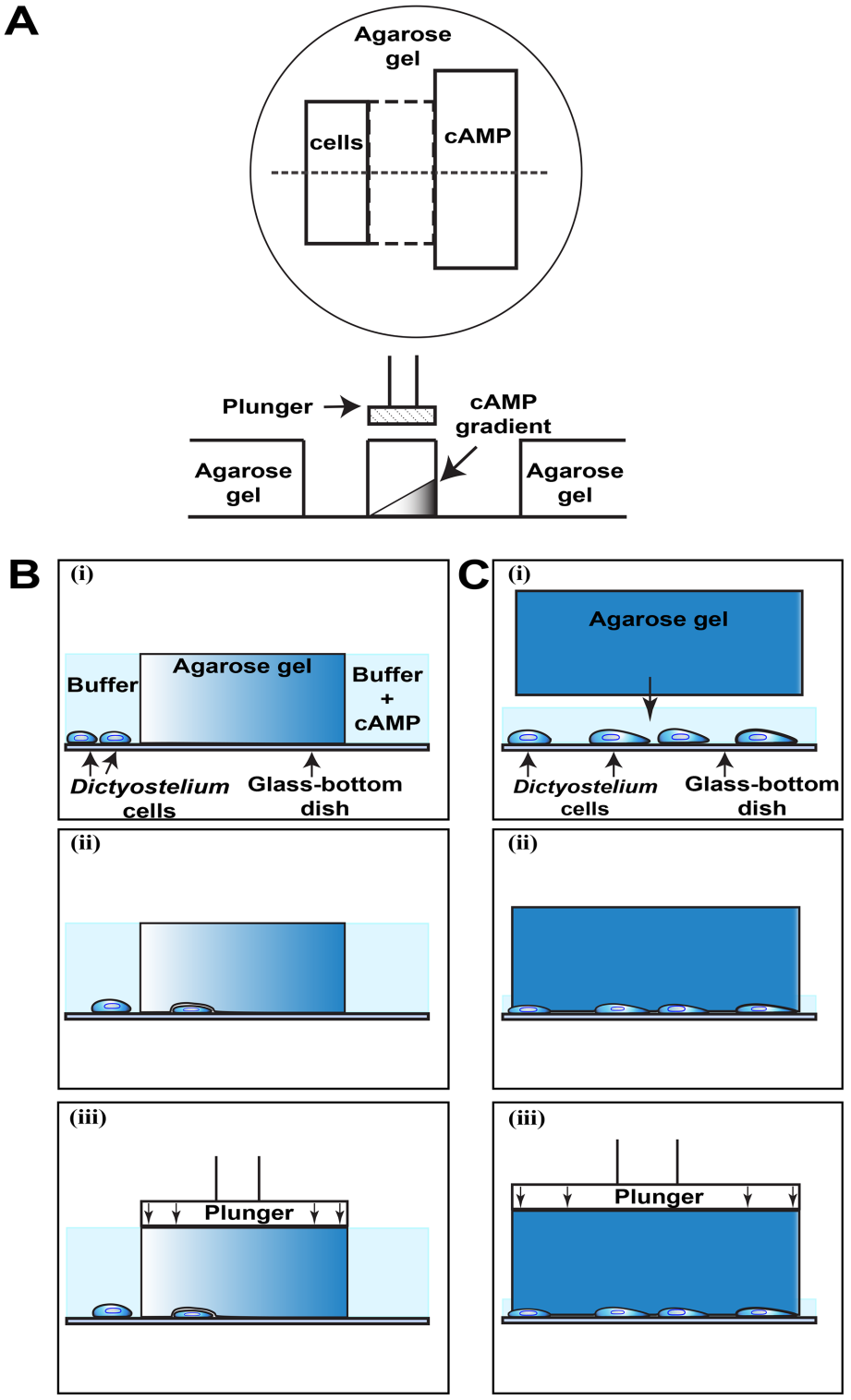

FIGURE 4: Two methods to place cells under agarose. (A, B) Cells attracted underneath an agarose gel by chemoattractant. (C) A layer of agarose placed on top of them.

To analyze quantitatively the transition observed in Figure 6, we show a record of both the load sensor signal and timing of bleb events for a particular experiment in Figure 7 (also see Supplemental Movie S3). The frequency of blebs strongly increases after the load is applied, with a first bleb triggered a few seconds after the compressive load starts to increase. After the load reaches its steady value of 400 Pa, up to six blebs are recorded over 1 min.

This establishes that the cell squasher influences the migratory behavior of cells by the imposition of a mechanical load alone and allows us to quantitatively study the transition.

DISCUSSION

We designed an automated device that accurately controls a mechanical compressive load at the interface between a migrating cell and a standard hydrogel such as agarose. Combining mechanical loading with live-cell imaging enables us to quantitatively analyze cells' response to mechanical perturbations. This was demonstrated by monitoring the morphological evolution and migration of *Dictyostelium* cells under compression. As an illustration of the system's capabilities, we present novel evidence that cells change their migratory behavior within seconds of the imposition of the load, getting flatter and transitioning from pseudopod- to bleb-based migration. Although a chemotactic cue is a convenient way to drive cells under an agarose overlay, similar results are also obtained by simply positioning the gel on top of nonchemotactic cells.

In addition to biological measurement, the same setup also provides a convenient method for characterizing hydrogel stiffness and creep behavior over relevant length and time scales. The Young's modulus values measured on the agarose gels used in the experiments are in excellent agreement with measurements made using an industry standard testing machine that many laboratories might not be able to afford or have access to. One attractive aspect of the setup presented here is therefore to provide a stand-alone rig to characterize both the mechanical properties of the environment and the response of the cells, with a total cost on the order of about $3000, largely due to the cost of the linear stage.

The reason why this system is simple is that the load is applied globally on the gel. This contrasts with more local manipulations, such as interactions with an atomic force microscope tip. Here we do not directly control the exact value of the load experienced by the cells under the agarose. In addition to the applied load, cells are likely to experience stresses due to the elastic deformation of the gel, which probably contribute to the remodeling of gel around them. The setup, however, is designed directly to control the key parameters of the cell's mechanical environment, stiffness, and load, such that comparison with in vivo conditions is possible.

The instrument is also generic enough to be used on other cell types and so reduce the dearth of tools that could be used to gather a quantitative understanding of mechanosensing response of cells performing their normal physiological functions.

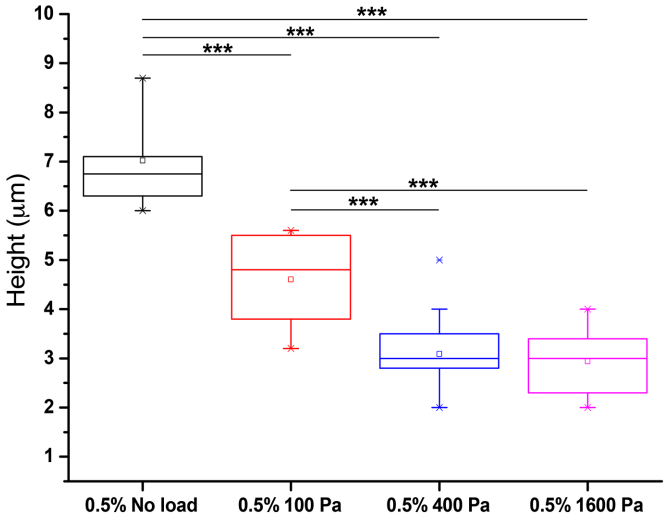

FIGURE 5: Cell height as a function of the imposed uniaxial load, under a gel of 0.5% agarose (20 cells for each case; $p < 0.001$; Tukey's means comparison test and one-way ANOVA).

Given that *Dictyostelium* cells are among the fastest cells, there is no doubt that many other cell types, including mammalian cells, could be studied without additional technical difficulties, besides perhaps tuning the range of forces sensed and applied. The setup would be useful to study, for instance, the migration of neutrophils in order to gain quantitative understanding about the immune response or cancer cell invasion under mechanical constraints (Friedl and Alexander, 2011). Coupling such measurements with the activity of mechanosensing pathways such as YAP/TAZ is likely to contribute to our understanding of mechanotransduction and its dynamics during individual or collective cell migration.

MATERIALS AND METHODS

Measurement of the Young's modulus of agarose gels

The Young's modulus of agarose gels was measured by indentation tests. The gels were prepared as 5-mm-thick agarose slabs of concentrations 0.5, 0.75, 1, 1.5, and 2% (wt/vol). Indentation tests were performed with the velocity of the bead movement set at 0.012 mm/s. A round steel bead of diameter of 6 ± 0.01 mm was used as an indenter.

The Young's moduli of the gels were also measured using a commercially available indentation instrument (5544; Instron, Canton, MA). Spherical indentation tests were performed on these gels to measure their stiffness.

The values were obtained as load–extension curves and used to calculate the Young's modulus of the agarose gel using the Hertz model by considering a nonadhesive elastic contact between the agarose gel and the indenting spherical bead (Hertz, 1882).

Cell culture and reporters

Experiments were done using the axenic strain Ax2 (Kay laboratory strain; DBS0235521 at http://dictybase.org) of *D. discoideum*. Cells were grown at 22°C in HL5 axenic medium in suspension.

D. discoideum was transformed with a F-actin reporter, ABD-GFP, to visualize protrusions. This reporter consists of ABP-120's F-actin domain (residues 9–248) fused to GFP and driven by a strong actin-15 promoter (Pang *et al.*, 1998); transformation of Ax2 with this reporter gave strain HM2040. Selection pressure was maintained by

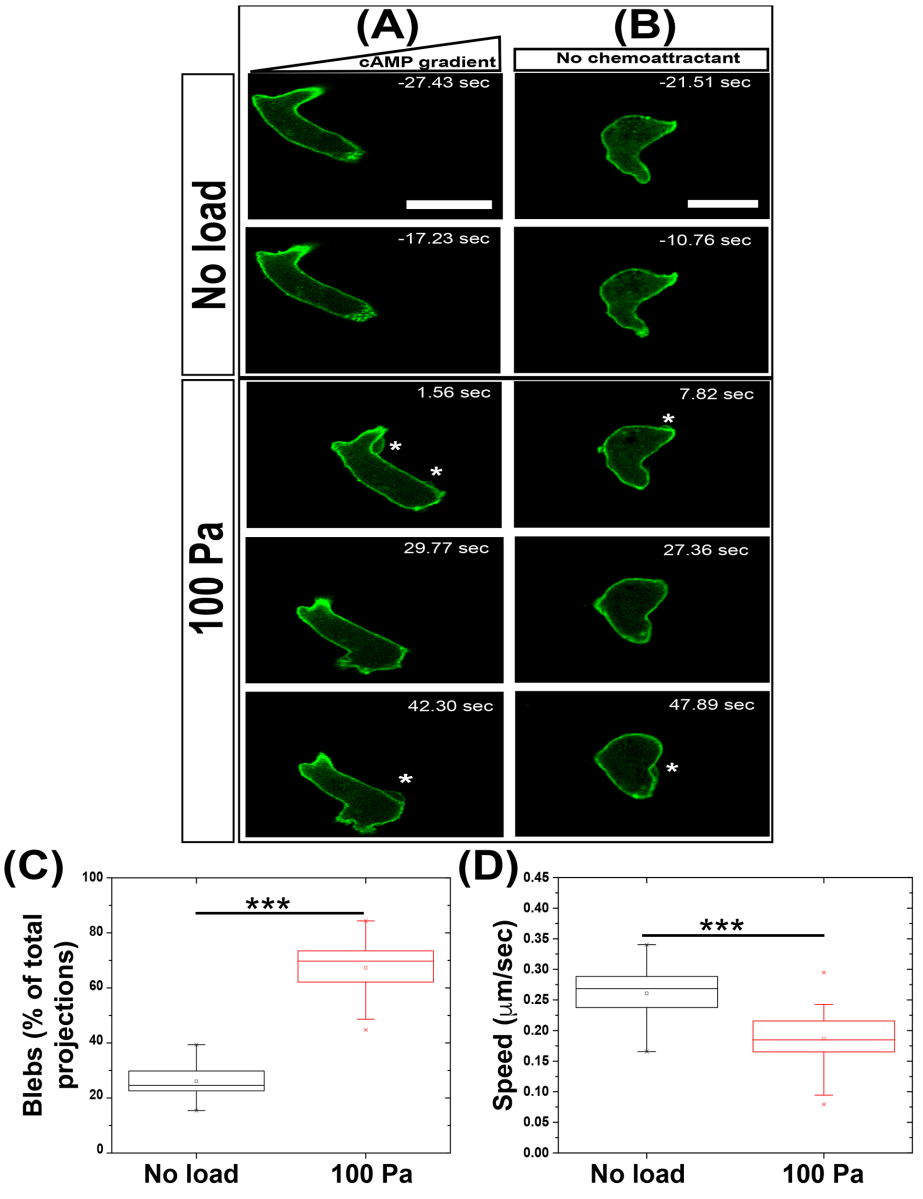

FIGURE 6: Protrusion formation of cells upon dynamic loading. Dynamic behavior of cells when migrating (A) along a chemotactic gradient or (B) without a gradient. *Dictyostelium* cells express ABD-GFP. The time indicated on each image is relative to the time at which the plunger makes contact with the 0.5% agarose gel. The imposed load is 100 Pa. Asterisks highlight the location of blebs on each image. (C, D) Quantification of blebs as proportion of total protrusions formed by cells and speed of migrating cells (≥20 cells for each condition; $p < 0.0001$; Tukey's means comparison test and one-way ANOVA).

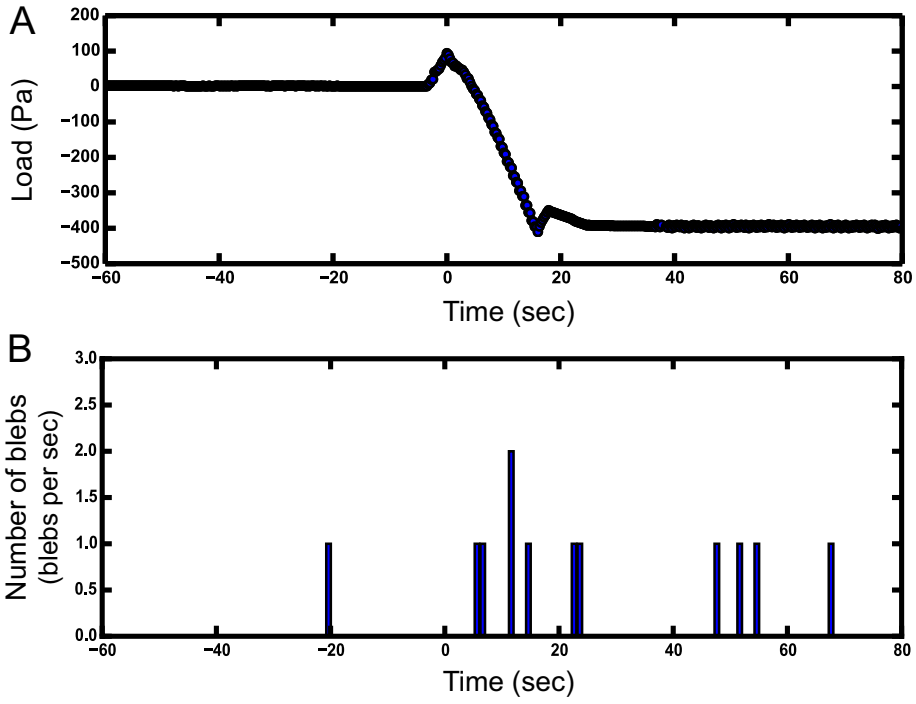

FIGURE 7: Quantitative analysis of the dynamic response of *Dictyostelium* cells to uniaxial loading. (A) Record of mechanical load as a function of time. Time $t = 0$ corresponds to the moment when the plunger makes contact with the gel. (B) Occurrence of blebs as a function of time. Representative data for a single cell migrating under 0.5% agarose and corresponding measurement from the cell squasher while applying a 400-Pa load.

growing the cells in medium containing 10 µg/ml G-418 antibiotic. This allowed selection for cells expressing this vector.

Preparation of cells for under-agarose and squashing experiments

KK2 buffer (16.5 mM KH_2PO_4, 3.8 mM K_2HPO_4, 2 mM $MgSO_4$, and 0.1 mM $CaCl_2$) was used as a standard buffer for all of the experiments. Aggregation-competent *Dictyostelium* cells were used for these assays. They were prepared by harvesting vegetative cells in exponential phase of growth. We resuspended 2×10^7 cells/ml in KK2; they were shaken at 180 rpm and 22°C for 1 h and then pulsed with 90 nM (final concentration after pulsing) cAMP every 6 min for a further 4.5 h. Cells stick to the glass walls and form small clumps upon reaching the stage of aggregation competency.

Microscopy and image analysis

Cells were imaged on a glass-bottom dish (35-mm dish with 10-mm glass bottom; MatTek) using an inverted laser-scanning confocal microscope (LSM780 or 710; Carl Zeiss) with a 63x/1.4 numerical aperture oil immersion objective. Images were collected using Zen 2010 software (Carl Zeiss) and processed using ImageJ (National Institutes of Health, Bethesda, MD).

Cell height was measured by reconstruction of *z*-stacks (0.4-µm increments) using Imaris (Bitplane). The *z*-axis elongation, partially due to mismatch in refractive indices (Hell *et al.*, 1993), was determined by comparing the *z*- and *x*/*y*-axes of fluorescent beads (9.7-µm-diameter FluoSpheres; Molecular Probes) and corrected by dividing stack increments by 1.97 (giving true *z*-axis increments of 0.203 µm).

Blebs are fast projections initially devoid of F-actin and were distinguished from the pseudopods using morphological evidence of an actin scar left behind when a bleb is formed. These projections were also distinguished using a kymograph by measuring rate of membrane projections. Numbers of blebs and pseudopods formed by a cell were counted, and the ratio of blebs and total projections was calculated.

The speed of cells was calculated by automated tracking using QUIMP plug-in in ImageJ (Tyson *et al.*, 2010). The centroid of cells was tracked at every frame of the movie to calculate the total distance covered by the cell. It was then divided by total time to calculate the speed of the cells.

Statistical analysis of the cell height measurement and speed of cells was done using one-way analysis of variance (ANOVA) and Tukey's means comparison test in Origin software (OriginLabs).

Cell migration assays

A modified version of the under-agarose assay was used (Laevsky and Knecht, 2001) to attract cells under the agarose as previously mentioned in (Zatulovskiy *et al.*, 2014). Briefly, 0.5% (wt/vol) SeaKem GTG agarose (Lonza Biochemicals) prepared in KK2 was poured into a preheated glass-bottom dish (35-mm dish with 10-mm glass bottom) to a height of 2 mm. Two parallel rectangular troughs were cut 4 mm apart once the agarose gel had cooled and set. The larger trough was 4 mm wide and 8 mm long, and the smaller one was 1 mm wide and 5 mm long. cAMP at 5 µM was added and left for ~30 min to allow a gradient of chemoattractant to be set up within the agarose layer, after which aggregation-competent cells were placed in the smaller trough. The load was applied using the device once the cells started to migrate under the agarose overlay.

The compressive load could also be applied on the cells without subjecting them to an under-agarose assay or chemotactic gradient, as shown in Figure 4C. Briefly, a 2-mm-thick agarose gel (0.5% [wt/vol]) was prepared in a glass-bottom dish. A suspension of aggregation-competent cells was placed in another glass-bottom dish. Once the agarose gel solidified, it was carefully lifted and placed over the cells. The load was subsequently applied on these cells.

To apply the load using the device, first the plunger was carefully brought close to the surface of the gel by manual positioning using the micrometers, and then the command to apply the desired load was given. A log file recorded the applied load at all the instances and was used for further data analysis. Quantitative analysis of the number of blebs corresponding to an applied mechanical load was done by measuring the number of blebs in cell migration movies and corresponding data of applied load from the log file of the device.

ACKNOWLEDGMENTS

We thank the workshop unit at the Department of Engineering and MRC Laboratory of Molecular Biology. We are also grateful to N. Barry for help with microscopy and D. Traynor for help and support in assembling the device and incorporating it with the microscope. This work is supported by a Dr. Manmohan Singh Scholarship from St. John's College to N.S., Medical Research Council Core Funding MC_U105115237 to R.R.K., and Biotechnology and Biological Sciences Research Council Grant BB/K018175/1 to A.J.K.

REFERENCES

Abu Shah E, Keren K (2013). Mechanical forces and feedbacks in cell motility. Curr Opin Cell Biol 25, 550–557.

Ahearne M, Yang Y, El Haj AJ, Then KY, Liu KK (2005). Characterizing the viscoelastic properties of thin hydrogel-based constructs for tissue engineering applications. J R Soc Interface 2, 455–463.

Alberts B, Johnson A, Lewis J, Raff M, Roberts K, Walter P (2002). Molecular Biology of the Cell, New York: Garland.

Bao G, Suresh S (2003). Cell and molecular mechanics of biological materials. Nat Mater 2, 715–725.

Bergert M, Chandradoss SD, Desai RA, Paluch E (2012). Cell mechanics control rapid transitions between blebs and lamellipodia during migration. Proc Natl Acad Sci USA 109, 14434–14439.

Bonnans C, Chou J, Werb Z (2014). Remodelling the extracellular matrix in development and disease. Nat Rev Mol Cell Biol 15, 786–801.

Bufi N, Durand-Smet P, Asnacios A (2015). Single-cell mechanics: the parallel plates technique. Methods Cell Biol 125, 187–209.

Charras G, Sahai E (2014). Physical influences of the extracellular environment on cell migration. Nat Rev Mol Cell Biol 15, 813–824.

Chen CS, Tan J, Tien J (2004). Mechanotransduction at cell-matrix and cell-cell contacts. Annu Rev Biomed Eng 6, 275–302.

Dai J, Ping Ting-Beall H, Hochmuth RM, Sheetz MP, Titus MA (1999). Myosin i contributes to the generation of resting cortical tension. Biophys J 77, 1168–1176.

Denais CM, Gilbert RM, Isermann P, McGregor AL, te Lindert M, Weigelin B, Davidson PM, Friedl P, Wolf K, Lammerding J (2016). Nuclear envelope rupture and repair during cancer cell migration. Science 352, 353–358.

De Vlaminck I, Dekker C (2012). Recent advances in magnetic tweezers. Annu Rev Biophys 41, 453–472.

Discher DE, Janmey P, Wang YL (2005). Tissue cells feel and respond to the stiffness of their substrate. Science 310, 1139–1143.

DuFort CC, Paszek MJ, Weaver VM (2011). Balancing forces: architectural control of mechanotransduction. Nat Rev Mol Cell Biol 12, 308–319.

Eyckmans J, Boudou T, Yu X, Chen CS (2011). A hitchhiker's guide to mechanobiology. Dev Cell 21, 35–47.

Field J, Swain M (1993). A simple predictive model for spherical indentation. J Mater Res 8, 297–306.

Friedl P, Alexander S (2011). Cancer invasion and the microenvironment: plasticity and reciprocity. Cell 147, 992–1009.

Friedl P, Gilmour D (2009). Collective cell migration in morphogenesis, regeneration and cancer. Nat Rev Mol Cell Biol 10, 445–457.

Gardel ML, Schneider IC, Aratyn-Schaus Yvonne, Waterman CM (2010). Mechanical integration of actin and adhesion dynamics in cell migration. Annu Rev Cell Dev Biol 26, 315–333.

Ghassemi S, Meacci G, Liu S, Gondarenko AA, Mathur A, Roca-Cusachs P, Sheetz MP, Hone J (2012). Cells test substrate rigidity by local contractions on submicrometer pillars. Proc Natl Acad Sci USA 109, 5328–5333.

Harris AK, Wild P, Stopak D (1980). Silicone rubber substrata: A new wrinkle in the study of cell locomotion. Science 208, 177–179.

Hell SW, Reiner G, Cremer C, Stelzer EHK (1993). Aberrations in confocal fluorescence microscopy induced by mistakes in refractive index. J Microsc 169, 391–405.

Hertz H (1882). Ueber die beruhrung fester elastischer korper. J Reine Angew Math 1882, 156–171.

Houk AR, Jilkine A, Mejean CO, Boltyanskiy R, Dufresne ER, Angenent SB, Altschuler SJ, Wu LF, Weiner OD (2012). Membrane tension maintains cell polarity by confining signals to the leading edge during neutrophil migration. Cell 148, 175–188.

Kay RR, Langridge P, Traynor D, Hoeller O (2008). Changing directions in the study of chemotaxis. Nat Rev Mol Cell Biol 9, 455–463.

Kim DH, Seo CH, Han K, Kwon KW, Levchenko A, Suh KY (2009). Guided cell migration on microtextured substrates with variable local density and anisotropy. Adv Funct Mater 19, 1579–1586.

King JS, Veltman DM, Insall RH (2011). The induction of autophagy by mechanical stress. Autophagy 7, 1490–1499.

Krishnan R, Park CY, Lin YC, Mead J, Jaspers RT, Trepat X, Lenormand G, Tambe D, Smolensky AV, Knoll AH, *et al.* (2009). Reinforcement versus fluidization in cytoskeletal mechanoresponsiveness. PLoS One 4, e5486.

Laevsky G, Knecht DA (2001). Under-agarose folate chemotaxis of *Dictyostelium discoideum* amoebae in permissive and mechanically inhibited conditions. Biotechniques 31, 1140–1149.

Lam RHW, Weng S, Lu W, Fu J (2012). Live-cell subcellular measurement of cell stiffness using a microengineered stretchable micropost array membrane. Integr Biol (Camb) 4, 1289–1298.

Lämmermann T, Sixt M (2009). Mechanical modes of "amoeboid" cell migration. Curr Opin Cell Biol 21, 636–644.

Liu YJ, LeBerre M, Lautenschlaeger F, Maiuri P, Callan-Jones A, Heuze M, Takaki T, Voituriez R, Piel M (2015). Confinement and low adhesion induce fast amoeboid migration of slow mesenchymal cells. Cell 160, 659–672.

Martin P (1997). Wound healing–aiming for perfect skin regeneration. Science 276, 75–81.

Miller CJ, Davidson LA (2013). The interplay between cell signalling and mechanics in developmental processes. Nat Rev Genet 14, 733–744.

Nelson RD, Quie PG, Simmons RL (1975). Chemotaxis under agarose: a new and simple method for measuring chemotaxis and spontaneous migration of human polymorphonuclear leukocytes and monocytes. J Immunol 115, 1650–1656.

Neuman KC, Nagy A (2008). Single-molecule force spectroscopy: optical tweezers, magnetic tweezers and atomic force microscopy. Nat Methods 5, 491–505.

Nichols JM, Veltman D, Kay RR (2015). Chemotaxis of a model organism: progress with *Dictyostelium*. Curr Opin Cell Biol 36, 7–12.

Normand V, Lootens DL, Amici E, Plucknett KP, Aymard P (2000). New insight into agarose gel mechanical properties. Biomacromolecules 1, 730–738.

Paluch EK, Raz E (2013). The role and regulation of blebs in cell migration. Curr Opin Cell Biol 25, 582–590.

Pang KM, Lee E, Knecht DA (1998). Use of a fusion protein between GFP and an actin-binding domain to visualize transient filamentous-actin structures. Curr Biol 8, 405–408.

Raab M, Gentili M, de Belly H, Thiam HR, Vargas P, Jimenez AJ, Lautenschlaeger F, Voituriez R, Lennon-Dumenil AM, Manel N, *et al.* (2016). ESCRT III repairs nuclear envelope ruptures during cell migration to limit DNA damage and cell death. Science 352, 359–362.

Tozluoglu M, Tournier AL, Jenkins RP, Hooper S, Bates PA, Sahai E (2013). Matrix geometry determines optimal cancer cell migration strategy and modulates response to interventions. Nat Cell Biol 15, 1–14.

Traynor D, Kay RR (2007). Possible roles of the endocytic cycle in cell motility. J Cell Sci 120, 2318–2327.

Tyson R, Epstein D, Anderson K, Bretschneider T (2010). High resolution tracking of cell membrane dynamics in moving cells: an electrifying approach. Math Model Nat Phenom 5, 34–55.

Tyson RA, Zatulovskiy E, Kay RR, Bretschneider T (2014). How blebs and pseudopods cooperate during chemotaxis. Proc Natl Acad Sci USA 111, 11703–11708.

Vedula SRK, Leong MC, Lai TL, Hersen P, Kabla AJ, Lim CT, Ladoux B (2012). Emerging modes of collective cell migration induced by geometrical constraints. Proc Natl Acad Sci USA 109, 12974–12979.

Wolf K, Te Lindert M, Krause M, Alexander S, Te Riet J, Willis A, Hoffman RM, Figdor CG, Weiss SJ, Friedl P (2013). Physical limits of cell migration: control by ECM space and nuclear deformation and tuning by proteolysis and traction force. J Cell Biol 201, 1069–1084.

Zatulovskiy E, Tyson R, Bretschneider T, Kay RR (2014). Bleb-driven chemotaxis of *Dictyostelium* cells. J Cell Biol 204, 1027–1044.